Advances in Scanning Electrochemical Microscopy*

Plenary Lecture

Meral Arca, Allen J. Bard,† Benjamin R. Horrocks, Thomas C. Richards and David A. Treichel

Department of Chemistry and Biochemistry, The University of Texas at Austin, Austin, TX 78712, USA

The basic principles of scanning electrochemical microscopy are discussed. Recent applications of this technique to studies of fast heterogeneous and homogeneous reactions and processes occurring in thin films (AgBr, polymers) are described. The use of novel scanning probes, *e.g.*, ion-selective electrodes and enzyme electrodes, is also discussed.

Keywords: *Electrochemistry; ultra microelectrode; scanning probe microscopy; imaging*

Introduction

Scanning electrochemical microscopy (SECM) involves the use of a small electrode moved very near a surface in an electrochemical cell arrangement to obtain information about the surface topography and reactivity and about reactions that occur in the solution space between tip and sample. Because there have been several recent extensive reviews of SECM,[1–4] this paper will stress the basic concepts of the technique in a rather non-mathematical way and will review recent applications.

Principles

Consider first the behaviour of a very small working electrode in an electrochemical cell. For example, suppose the electrode is a small sphere (*e.g.*, a hanging drop of mercury) with a radius, a, of a few micrometres. When this electrode is made the working electrode in an electrochemical cell containing a reducible species, O, and a sufficiently negative potential is applied to the electrode such that the reaction occurs at a diffusion-controlled rate, the current flowing through this electrode will be given by[5]

$$i = nFAc_O^*D_O\left[(\pi D_O t)^{-1/2} + a^{-1}\right] \quad (1)$$

where n is the number of electrons in the electrode reaction, F the Faraday constant, A the electrode area, c_O^* the bulk concentration of the oxidized species, D_O the diffusion coefficient of the oxidized species and t the time. The two terms on the right-hand side of eqn. (1) represent the transient response when all of the reaction occurs very near the electrode surface and a steady-state term which becomes important at longer times. Clearly, when $a^{-1} \gg (\pi D_O t)^{-1/2}$, or $t \gg a^2/\pi D_O$, a steady-state current, i_{SS}, results, with a value

$$i_{SS} = 4\pi nFD_Oc_O^*a \quad (2)$$

where the area of a sphere, $A = 4\pi a^2$, has been substituted into eqn. (1). A similar equation holds for a small disc electrode, (an ultramicroelectrode, UME), *e.g.*, constructed by sealing a small Pt wire of radius a into a drawn-out glass capillary tube.[6] Most SECM experiments are conducted with such disc-shaped UMEs (often called 'tips') where the steady-state current, when the tip electrode is far from any surface, is given by[6]

$$i_{T,\infty} = 4nFD_Oc_O^*a \quad (3)$$

This steady-state current represents the diffusive flux of O to the electrode from the bulk solution. The SECM response is based on how the current to this UME tip is perturbed by the presence of a substrate near the tip[7] (Fig. 1). When the tip is brought near an inert non-conductive surface (such as a piece of glass), the current will be smaller than the $i_{T,\infty}$ of eqn. (3), because the surface blocks the diffusive flux of O to the tip. The closer the tip is to the surface, the smaller the current, until, when the tip-to-surface spacing, d, becomes zero, the tip current will approach zero. An equation for the tip current, i_T, as a function of d for this situation that holds fairly well is[8]

$$(i_T/i_{T,\infty}) = [0.292 + 1.515/L + 0.655\exp(-2.4035/L)]^{-1} \quad (4)$$

where the normalized tip–substrate separation $L = d/a$. Thus the presence of a non-reactive substrate near the tip can always be recognized by the condition $i_T < i_{T,\infty}$.

A different behaviour is observed when the tip is near a surface where tip-generated product R can be oxidized back to O, *e.g.*, when the substrate is a conductive material at a sufficiently positive potential. In this instance, there is a flux of O to the tip from the substrate in addition to that from the bulk solution. Due to this positive feedback from the substrate, $i_T > i_{T,\infty}$. When the reaction of R to O occurs at the surface at a diffusion-controlled rate, the following equation applies:[8]

$$(i_T/i_{T,\infty}) = 0.68 + 0.7838/L + 0.3315\exp(-1.0672/L) \quad (5)$$

Plots of $i_T/i_{T,\infty}$ for the two cases governed by eqns. (4) and (5) are shown in Fig. 2. Note that these equations and the plots in Fig. 2 are in the form of dimensionless parameters i_T (= $i_T/i_{T,\infty}$) and L (= d/a). Thus, if a is known, then these equations can be used to determine d, independent of the magnitudes of c_O^* and D_O, from the measured tip currents.

Imaging With SECM

A topographic image of a sample can be obtained by moving the tip towards the substrate, until i_T is perturbed by its presence, and then moving the tip in a plane parallel to the substrate surface (the xy-plane) and recording the changes in i_T as a function of the x,y position. This is accomplished by using a piezoelectric scanner driven by three programmable power supplies, as in other types of scanning probe microscopy. A potentiostat controls the potential of the tip and, if necessary, the substrate. The scanning, potentials and current measurement are controlled by a computer which later can be

* Presented at EIRELEC '93, Electrochemistry to the year 2000, Adare, Co. Limerick, Ireland, September 11–15, 1993.

† To whom correspondence should be addressed.

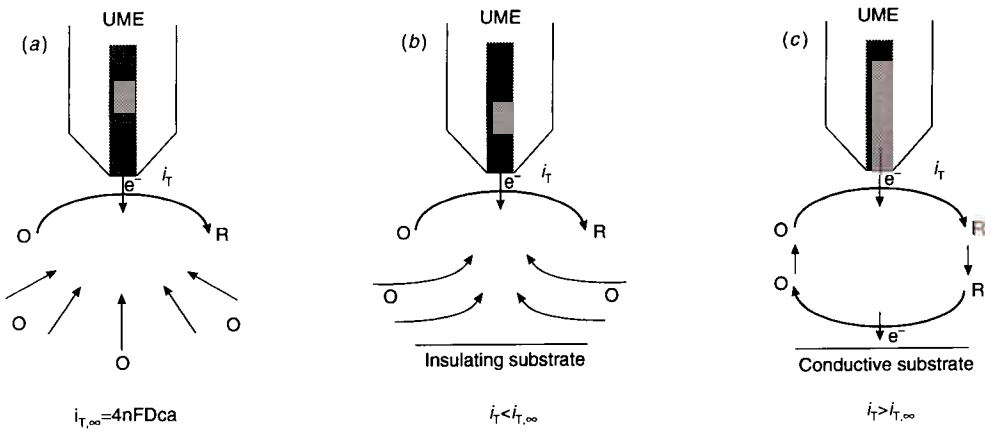

Fig. 1 Basic principles of SECM. (*a*) With UME far from the substrate, diffusion of O leads to a steady-state current, $i_{T,\infty}$. (*b*) With UME near an insulating substrate, hindered diffusion of O leads to $i_T < i_{T,\infty}$. (*c*) With UME near a conductive substrate, positive feedback of O to the tip leads to $i_T > i_{T,\infty}$

used for processing and displaying the results. Details of the SECM apparatus and tip construction are given elsewhere.[1] By relating i_T to $i_{T,\infty}$, one can determine which zones on the substrate are conductive and which are insulating. This information can also be obtained without knowledge of $i_{T,\infty}$ by tip-position modulation,[10] where the tip is moved up and down with a sinusoidal motion and variations in i_T are noted. The resolution obtainable in SECM is governed by the size of the tip and is currently of the order of 50 nm. Typical SECM images are shown in Figs. 3 and 4.

Determination of Heterogeneous Electron-transfer Kinetics

SECM has recently emerged as a useful technique for the measurement of the rate constants of fast heterogeneous electron-transfer reactions.[11,12] For these measurements, the SECM apparatus is used to form a twin-electrode thin-layer cell between the microelectrode tip and a conducting substrate. During voltammetric scans, this configuration induces high rates of mass transfer between the substrate and tip electrodes owing to the large concentration gradients existing between the two closely spaced electrodes generating complementary forms of a redox couple. As the over-all rate of an electron transfer (represented by i_T) can be limited by either the rate of mass transfer to the electrode or the intrinsic heterogeneous electron-transfer rate, this increase in mass transfer allows faster rates of electron-transfer processes to be measured in the SECM arrangement than can be accomplished with the same electrode in bulk solution.

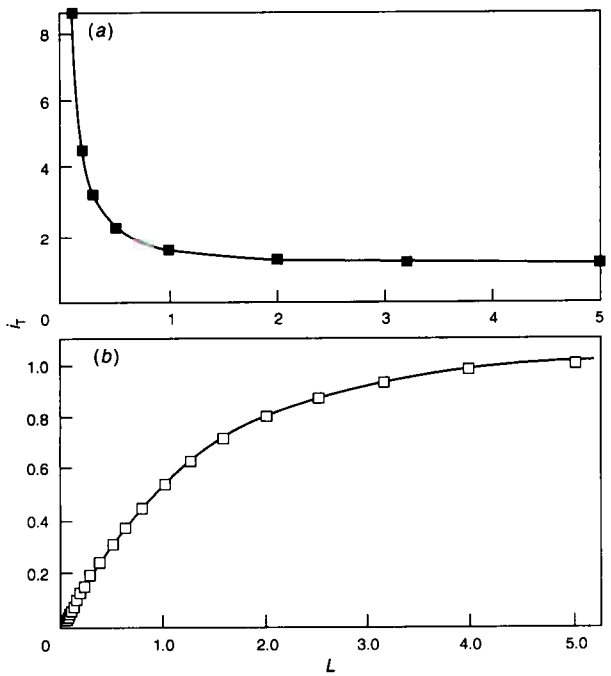

Fig. 2 Diffusion-controlled steady-state tip current as a function of tip–substrate separation. $i_T = i_T/i_{T,\infty}$; $L = d/a$. (*a*) Substrate is a conductor; solid line calculated from eqn. (5). (*b*) Substrate is an insulator; solid line calculated from eqn. (4). Squares are experimental data from ref. 9

In general, an electrochemical technique is sensitive to the intrinsic heterogeneous electron-transfer rate whenever the mass-transfer coefficient, m, is of the same order of magnitude or greater than the standard heterogeneous electron-transfer rate constant, k^o. For diffusion-controlled transient techniques, m is approximately $(D/t)^{1/2}$ (D = diffusion coefficient); hence short timescale experiments are required to increase m to levels needed to determine k^o. These transient measurements are often complicated by the need for sophisticated instrumentation to measure currents at short times and by interference from capacitive currents and by currents due to adsorbed electroactive species. For steady-state processes, increased mass transfer is achieved by altering electrode geometries or configurations (*e.g.*, decreasing a) to generate large concentration gradients and thus strong driving forces for mass transfer near the electrode.

The advantages of SECM can be seen by comparing mass-transfer coefficients for two different electrode configurations. For a microdisc electrode in bulk solution, the steady-state mass-transfer coefficient is given by[6,13,14] m is approximately D/a (the smallest value of a at present for well-defined and characterizable electrode geometries is about 500 nm). For a thin-layer configuration,[12,15,16] m is approximately D/d. To date, the thinnest stable layers achieved are about 40 nm thick for a 1 μm diameter Pt disc electrode opposed by a liquid (mercury) substrate. Clearly, the rate of mass transfer can be enhanced by more than an order of magnitude in going from a microelectrode in bulk solution to the thin-layer configuration in SECM.

As mentioned above, recent experimental work[11,17] has demonstrated that thin stable layers of solution can be maintained between an SECM microelectrode tip and a mercury substrate as illustrated in Fig. 5, although SECM measurements with solid substrates are also possible. Recent theory[16] has been developed to extract kinetic parameters

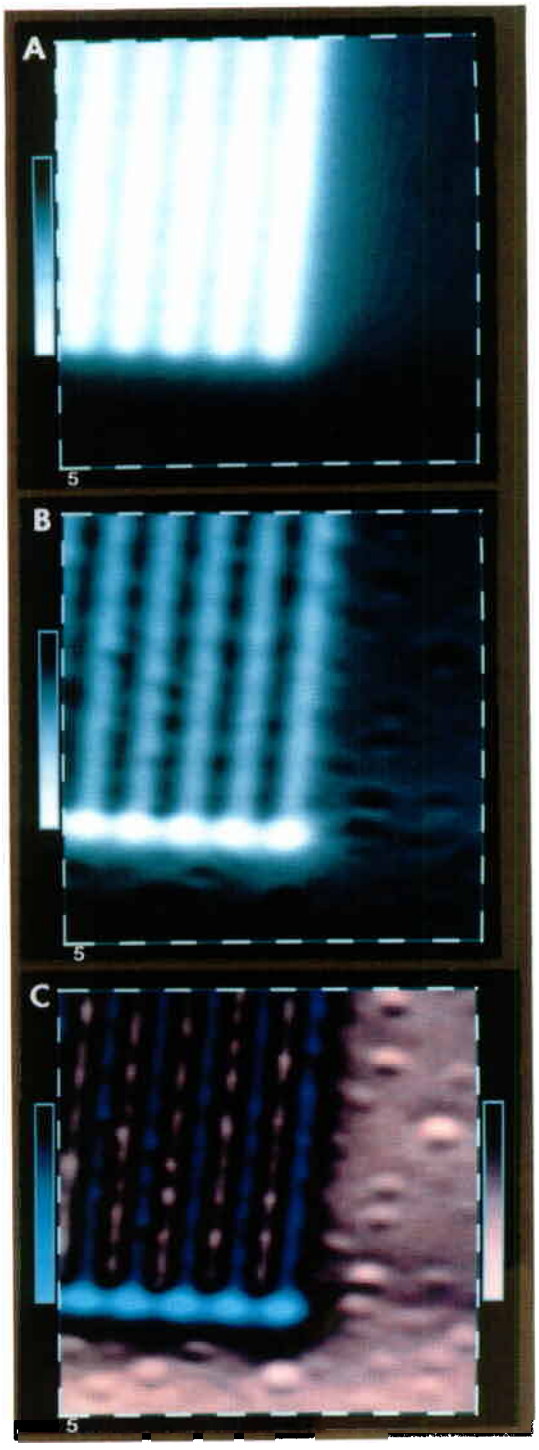

Fig. 3 SECM and tip position modulated (TPM) SECM images of an interdigitated array electrode (IDA). 5 μm wide Pt bands spaced by 5 μm SiO$_2$. The upper left part of each image shows a portion of the IDA and the remainder of the image is the insulating SiO$_2$ substrate. (*a*) Direct current SECM image. (*b*) TPM SECM image. (*c*) Absolute value TPM SECM image. The images in (*a*) and (*b*) show more positive current as a lighter shade, hence the apparent crater like features are actually bumps. Using the absolute value of the TPM in phase current allows separate colour scales for insulating and conducting regions and results in a more conventional representation of the surface topography. Reprinted from ref. 10 with permission. Copyright American Chemical Society.

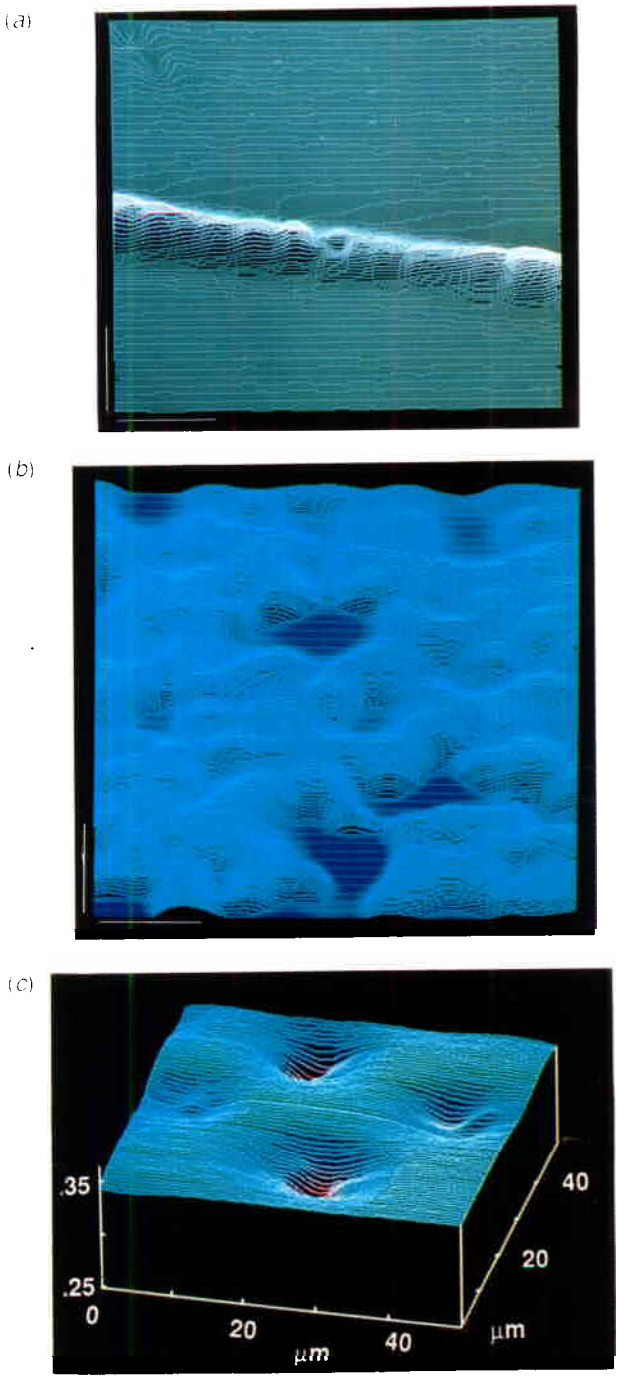

Fig. 4 (*a*) SECM image of a filament of blue green algae (*Oscillatoria*). Scale bars = 10 μm. Individual cells of the filament are apparent from the indentations that indicate cell wall junctions. The cell size indicated by SECM is consistent with that determined by optical microscopy. (*b*) Positive feedback SECM image of an electrochemically conductive silver filter membrane (small silver particles that have been sintered to form a porous film with an average pore size of approximately 5 000). Scale bars = 10 μm. (*c*) SECM line scan image of enzymically active rat liver mitochondria immobilized on glass. Over glass regions, the image is flat, indicating negative feedback caused by the insulating surface. Over mitochondria, the image is blurred owing to the large size of the tip (8 μm diameter carbon fibre) relative to the dimensions of the mitochondria. The decreased current response at the perimeter of each mitochondrion is indicative of its surface relief, which partially blocks diffusion of the mediator to the tip. Vertical axis is z/a. Images reprinted from ref. 5 with permission. Copyright American Association for the Advancement of Science.

(m,k^0) relatively simply from steady-state cyclic voltammograms, and this approach can be used for microelectrode tips either in bulk solution or in a thin-layer SECM configuration utilizing either solid or liquid substrates. Fig. 6 shows theoretical curves illustrating the effect of changing the value of k^0 for a steady-state voltammogram in a thin-layer configuration. As shown, the voltammetric wave broadens as the heterogeneous electron-transfer rate decreases and kinetic information is easily extracted from voltammograms when $k^0/m < 5$.

With respect to specific chemical systems, thin-layer SECM has been used to measure k^0 for the reduction of C_{60} at a mercury substrate[11] and for the oxidation of ferrocene (one of the fastest heterogeneous electron-transfer processes known) at a platinum substrate.[12] Fig. 7 shows experimental data overlaid with theoretical calculations for the ferrocene system taken at different tip–substrate separations. Here, as the tip–substrate separation decreases, the limiting current increases and the wave broadens owing to the rate of mass transfer and consequential sensitivity to faster intrinsic electron-transfer rates. The measured k^0 in this instance was 3.7 ± 0.6 cm s^{-1}.

Homogeneous Chemical Reactions

SECM can also be used to measure the rate of homogeneous chemical reactions that are associated with an electrochemical oxidation or reduction. In this application, the tip and substrate electrodes are analogous to the ring and disc electrodes in a rotating ring–disc electrode,[18] or to the walls in a thin-layer electrode.[15] To date, experimental studies have been conducted and theoretical treatments developed for both first- and second-order homogeneous chemical reactions following the electron-transfer step.[19,20] The primary focus of this section will be on recent studies of second-order reactions.

A representative reaction scheme which can be studied by SECM is

tip: $R \rightarrow O + ne^-$
gap: $2O \rightarrow$ products
substrate: $O + ne^- \rightarrow R$

This scheme differs from that described under Principles in that products diffusing from the tip can react in the gap to form electroinactive species before reaching the substrate. This loss of O reduces both the collection current measured at the substrate (i_S) and the feedback current measured at the tip (i_T).

Theoretical working curves, *viz.*, current *versus* tip–substrate separation, showing the effect of second-order homogeneous reactions are illustrated for both tip feedback ($i_T/i_{T,\infty}$) and substrate collection ($i_S/i_{T,\infty}$) *versus* d (Fig. 8). The normalized (or dimensionless) rate constant, K, is related to the dimerization rate constant, k_2, by the relationship $k_2 = KD/a^2c_O^*$. The curve for a reaction with $K = 0$ represents the behaviour observed for a stable, reversible couple cycled between a tip and substrate electrode. In this situation, at small tip–substrate separations, all of the oxidized material leaving the tip is reduced at the substrate and then cycled back to the tip (*i.e.*, the collection efficiency is 100% or $i_S/i_T \approx 1$). Likewise, the curve for an infinite rate constant is the same as that observed for a couple with stable O and R as the tip electrode approaches an insulating surface as discussed under Principles. In both instances, no feedback is observed and the tip current is reduced as diffusion to it becomes hindered. The central curves represent data for finite K values. In experimental studies, the values for the tip radii and the bulk concentrations are chosen to yield normalized rate constants in the range shown in Fig. 8.

Rate constants should be measurable if the tip and substrate are positioned sufficiently close that a detectable amount of R can cross the gap before reacting. For a reaction rate to be measurable, the time τ, required for a species to cross the gap is approximately d^2/D. As τ is approximately $1/k_2c_O^*$ for a

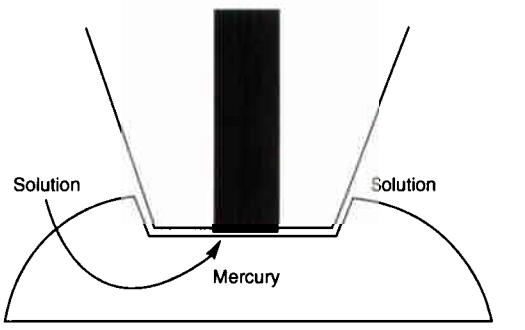

Fig. 5 Proposed scheme for the maintenance of thin layers of solution between a microelectrode tip and mercury substrate

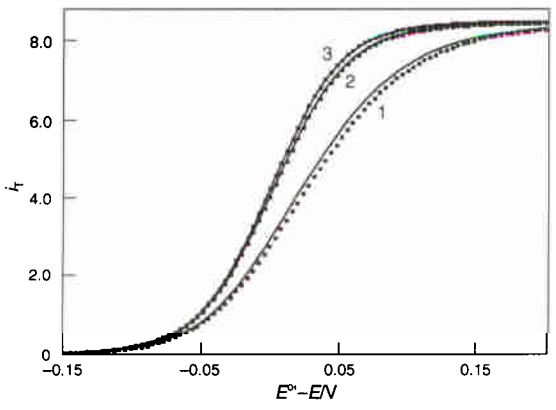

Fig. 6 Theoretical steady-state voltammograms for a thin-layer configuration. Two different approximations were implemented (squares for one approach, solid lines for the other) to produce *i versus E* curves. Here, the value of k^0 decreases in proceeding from curve 3 to curve 1. Currents are normalized such that i_T is the ratio of the tip current in the thin-layer configuration to that for the same electrode in bulk solution. Reprinted from ref. 12 with permission. Copyright American Chemical Society

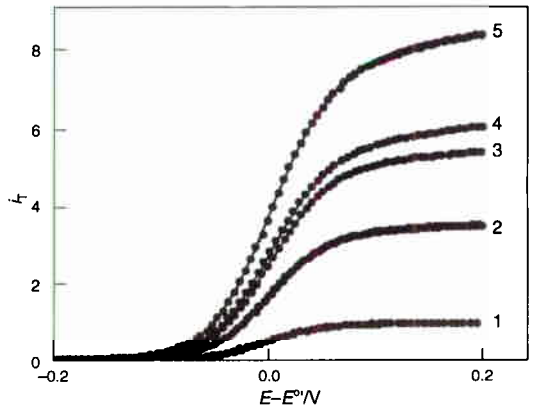

Fig. 7 Experimental data for the oxidation of ferrocene overlaid with theoretical calculations for a 2 μm diameter Pt tip opposed by a 1.5 mm diameter Pt substrate electrode. Voltammograms 1–5 show the transition from data recorded in bulk solution (curve 1) to those recorded with the tip electrode 100 nm from the substrate. Currents are normalized as in Fig. 6, and the *i versus E* curves characteristically broaden with enhanced currents as the rate of mass transfer increases in the thin-layer configuration. Reprinted from ref. 12 with permission. Copyright American Chemical Society

second-order reaction, the rate constant can be estimated as $k_2 \approx D/d^2c_O^*$. Representative values ($D = 10^{-5}$ cm^2 s^{-1}, $d = 200$ nm and $c_O^* = 2.5 \times 10^{-4}$ mol l^{-1}) indicate that rate constants of the order of 10^8 l mol^{-1} s^{-1} should be measurable. Similarly, for first-order kinetics $\tau = 1/k_1$ (k_1 = rate constant for homogeneous first-order reaction of tip-generated species), which should yield measurable rate constants as large as 10^5 s^{-1}.

In order to test the utility of SECM for measuring second-order kinetics, molecular systems with different rate constants have been chosen. The radical anion dimerizations of two activated alkenes, dimethyl fumarate and fumaronitrile, have been studied in *N*,*N*-dimethylformamide.[20] Rate constants of 170 and 2×10^5 l mol^{-1} s^{-1}, respectively, were calculated using both tip feedback and substrate current measurements. Good agreement of experiment with theory was seen for both modes of SECM operation.

More recently, research has been directed at extending the use of SECM to the study of even faster reactions, in particular, the dimerization of phenolates[21] and acrylonitrile.[22] 4-Nitrophenolate, which has been shown to undergo a fast irreversible dimerization following oxidation, was chosen for the first study.[23,24] Experimental curves for tip feedback are shown in Fig. 9. The calculated rate constant, approximately 8×10^7 l mol^{-1} s^{-1}, agrees favourably with that measured by fast-scan cyclic voltammetry.[23] The rate constant found for the dimerization of the acrylonitrile radical was $6 \pm 3 \times 10^7$ l mol^{-1} s^{-1}.[22]

Characterization of Thin Films

SECM can be used to characterize electrodes modified with electronically and ionically conductive polymers and also with non-electroactive thin coatings and films. By analysing the SECM approach curves, one can determine the diffusion coefficient of species inside the film, the heterogeneous rate constant for a chemical reaction at the film–solution interface and the site where any heterogeneous chemical or electrochemical reaction occurs. This methodology will be illustrated with AgBr films several micrometres thick, electrodeposited on a Ag substrate.[25] The Ag–AgBr substrates show negative feedback with $Os(bpy)_3^{2+}$ (bpy = 2,2′-bipyridyl) and positive feedback with $Ru(NH_3)_6^{3+}$ redox mediators (Fig. 10). As AgBr is highly resistive, the diffusion of both mediators to the Ag substrate is blocked by the AgBr layer. Negative feedback current was obtained with $Os(bpy)_3^{2+}$, because tip-generated $Os(bpy)_3^{3+}$ does not react with AgBr. The positive SECM feedback observed with $Ru(NH_3)_6^{3+}$ is due to chemical reaction with AgBr

$$Ru(NH_3)_6^{3+} + e^- = Ru(NH_3)_6^{2+} \text{ (tip process)} \quad (6)$$

$$AgBr + Ru(NH_3)_6^{2+} \xrightarrow{k} Ag + Br^- + Ru(NH_3)_6^{3+} \text{ (substrate process)} \quad (7)$$

The heterogeneous rate constant for this reaction, 0.082 cm s^{-1}, was extracted from approach curves obtained with

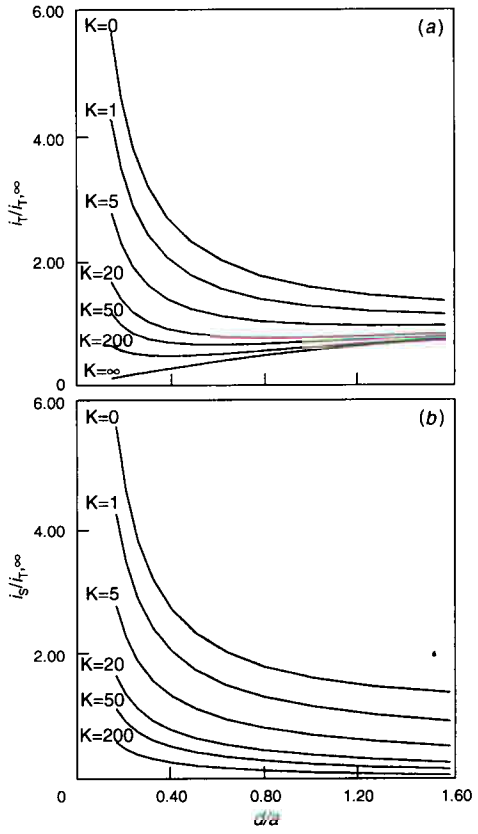

Fig. 8 Simulated tip and substrate electrode current–distance curves for different values of K. (*a*) Tip feedback. (*b*) Substrate collection. Both currents and distance are normalized

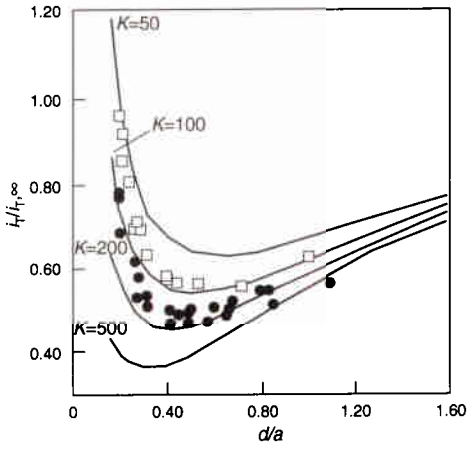

Fig. 9 Normalized tip current–distance behaviour for □, 0.2 and ●, 0.4 mmol l^{-1} 4-nitrophenolate; a = 2.5 μm

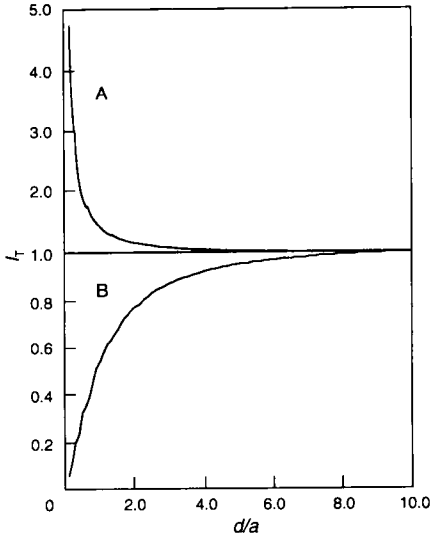

Fig. 10 SECM approach curves obtained with a 10 μm diameter Pt tip over a Ag–AgBr substrate. Scan rate, 0.1 μm s^{-1}. A, 10 μm AgBr, 5 mmol l^{-1} $Ru(NH_3)_6^{3+}$ in 0.5 mmol l^{-1} KNO_3, $E_T = -0.45$ V *versus* SCE. B, 2 μm AgBr, 2 mmol l^{-1} $Os(bpy)_3^{2+}$ in 0.5 mmol l^{-1} KN_3O, $E_T = +0.8$ V *versus* SCE

different thicknesses of an AgBr film. The diffusion coefficient of Br^- inside a AgBr layer could also be obtained by transient measurements. The tip was held at +0.9 V *versus* the saturated calomel electrode (SCE), where Br^- is oxidized, and a negative potential pulse was applied to the Ag–AgBr electrode, initiating the reduction of AgBr

$$AgBr + e^- = Ag + Br^- \text{ (substrate reaction)} \quad (8)$$

$$2Br^- \rightarrow Br_2 + 2e^- \text{ (tip reaction)} \quad (9)$$

The diffusion coefficient characterizing the speed of the Br^- movement in the AgBr lattice was found to be 5.6×10^{-7} $cm^2\ s^{-1}$, about 35 times smaller than the analogous value in aqueous solution.

The ejection and incorporation of ions from polymer-coated electrodes has been studied by SECM.[26–30] We have also used SECM to investigate the oxidation–reduction process of the electronically conductive polymer, poly(pyrrole) (PPy).[31] Anion expulsion or cation insertion can occur when PPy is switched electrochemically from the oxidized (conducting) to the reduced (insulating) states. These processes can be written as:

$$PPy^+A^- + e^- \rightarrow PPy^0 + A^-\ (aq) \quad (10)$$

$$PPy^+A^- + C^+\ (aq) + e^- \rightarrow PPy^0A^-C^+ \quad (11)$$

where PPy^+ and PPy^0 represent the oxidized and reduced forms of the polymer, respectively, A^- is the anion incorporated during PPy synthesis and C^+ is the cation of the supporting electrolyte. If A^- or C^+ is electroactive, one can determine the extent to which each of these processes occurs by using SECM. Fig. 11 shows the SECM tip collection/substrate generation cyclic voltammogram of a PPyBr film.[31] In order to monitor the ejection of Br^- from the polymer during reduction of the film, the tip electrode was positioned above the coated electrode and held at a potential of +0.9 V, where ejected Br^- would produce an anodic tip current. The SECM tip–substrate cyclic voltammogram and transient measurements showed that the relative importance of processes (10) and (11) depends on the potential during a cathodic scan of the PPy^+Br^-. In the region between 0.0 and −0.4 V, although the PPy^+Br^- is being reduced, Br^- expulsion, and hence the tip current, is small. In order to maintain electroneutrality in this region, cations (*e.g.*, K^+) must be inserted into the film. At more negative potentials, however, Br^- is released from the film and the tip current increases.

An even more intriguing way in which SECM can be used to study polymers is by moving a very small tip into the polymer film itself and recording the tip current as a function of tip penetration. Voltammograms (i_T *versus* E) (E = potential) can also be obtained with the tip inside the film. An example of this approach was the study of a 220 nm thick Nafion film containing $Os(bpy)_3^{3+}$, where i_T measurements allowed determination of film thickness, D, for $Os(bpy)_3^{3+}$, and k^o for the electron-transfer reaction.[32] We have recently carried out a similar study with a poly(vinylferrocene) film.[33]

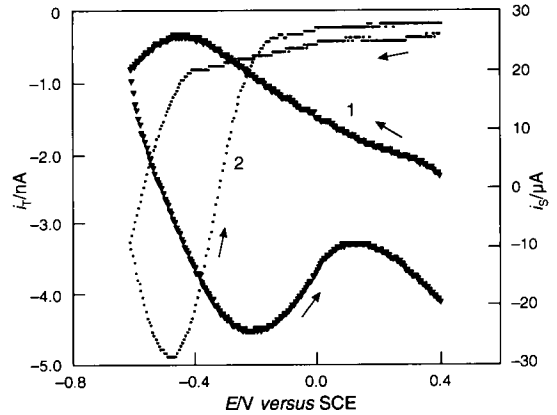

Fig. 11 SECM tip/substrate cyclic voltammogram of PPyBr film in 0.1 mol l^{-1} K_2SO_4 solution. E_T = +0.9 V *versus* SCE. Tip was positioned 5 μm above the substrate. 1, Substrate cyclic voltammogram. 2, Tip cyclic voltammogram

Novel Probes

Many interesting chemical systems are not accessible to voltammetric techniques and amperometric probes; for example, alkali metal cation concentrations and pH cannot be measured in this way. Direct voltammetric techniques have poor chemical selectivity and, therefore, it may be difficult to distinguish the current due to the analyte from that due to other electroactive species, *e.g.*, oxygen. Several approaches

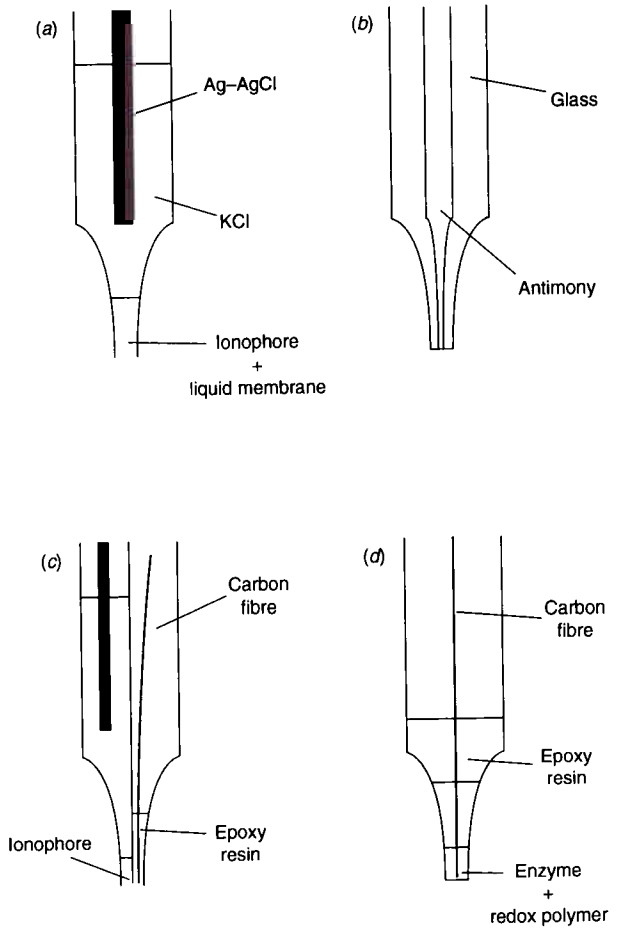

Fig. 12 (*a*) Liquid membrane micropipette type of ion-selective microelectrode used in physiology for potentiometric determination of alkali metal and alkaline earth metal cation activities. Minimum tip size approximately 0.2 μm. (*b*) Antimony in glass microdisc electrode used for potentiometric pH measurements in SECM. Minimum diameter of antimony disc approximately 1 μm. (*c*) Proposed dual function tip with liquid membrane potentiometric sensor for determination of cations and carbon microdisc for SECM feedback measurements. (*d*) Horseradish peroxidase biosensor used to measure hydrogen peroxide concentration profiles in SECM. Hydrogen peroxide in solution diffuses to the tip where it is reduced at the active site of the enzyme. The redox polymer serves to immobilize the enzyme and provides a path for electrons to the active site where they regenerate the reduced form of the enzyme. A typical tip diameter is 20 μm

to increasing the scope and selectivity of SECM are possible based on the use of novel probes such as potentiometric ion-selective microelectrodes and microscopic amperometric biosensors.

In the life sciences, potentiometric ion-selective microelectrodes of the type shown in Fig. 12(*a*) are routinely used for the measurement of intracellular pH and alkali metal and alkaline earth metal cation activities.[34] Halide ion-selective microelectrodes can also be prepared by anodizing silver microelectrodes in potassium halide solutions.[29] In principle, all of these microelectrodes can be used as the scanning probe in SECM. Chloride ion-selective probes have already been used to monitor chloride ion fluxes during the electrochemical switching of conductive polymers[29] and to obtain chloride concentration profiles at pits on corroding metals.[35] The application of pH-selective probes to the measurement of surface pH during corrosion of steel[35] and aluminium[36] and local pH profiles generated by water reduction, enzymic hydrolysis of urea, and the metabolism of glucose by yeast have also been reported.[37]

There are two important differences between the potentiometric SECM mode and voltammetric SECM. First, the tip is acting as a passive sensor and, therefore, local concentration profiles of the analyte must be generated at the surface under study. This decreases the resolution of the images with respect to voltammetric feedback SECM because diffusion is no longer confined to the tip–surface gap. The potentiometric mode of operation is, therefore, similar to substrate generation/tip collection experiments in voltammetric SECM. Second, in voltammetric SECM, the tip–surface distance can be accurately determined from the tip feedback current, whereas in potentiometric SECM, the tip is a passive sensor and no distance information is available. This presents the technical problem of how to bring the tip close to the surface. The use of a telescopic lens allows approximate positioning of the tip within a few micrometres of the surface; however, for quantitative measurements, a more accurate distance calibration is necessary. For antimony microdisc pH sensing tips [Fig. 12(*b*)], this can easily be solved by employing the tip as a voltammetric electrode and determining the distance from the feedback current before switching to potentiometric operation for the pH measurements. An example of a pH profile around an 80 μm diameter disc of yeast cells immobilized in agarose and imaged with an antimony tip is shown in Fig. 13. Near the centre of the disc (lower right-hand corner), the pH is lower than the bulk solution by approximately 0.5 pH unit because of the production of acidic metabolites by the yeast.

Unfortunately, the liquid membrane ion-selective microelectrodes cannot be used as voltammetric probes because of their very high internal resistance. However such probes could still be useful for qualitative studies of metal ion concentration profiles. Work is in progress to construct dual tips with one voltammetric probe and one ion-selective probe [Fig. 12(*c*)] where the voltammetric probe would be used to provide a distance calibration.

The poor chemical selectivity of voltammetric microelectrodes can be greatly improved by coupling them to enzymic reactions to produce an amperometric biosensor. Many different designs for microscopic amperometric biosensors have been reported and in principle all could be employed in SECM.[38–46] Recent work by this group has used the design in Fig. 12(*d*). This sensor detects hydrogen peroxide using an

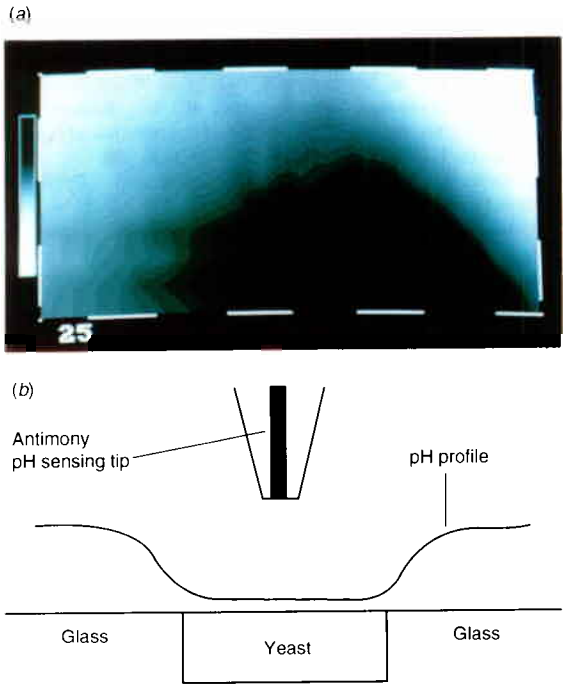

Fig. 13 Image of the pH profile around a section of an 80 μm diameter yeast–agarose disc.[37] Grey scale indicates the potential of the antimony tip; white corresponds to high pH. Tip diameter, 20 μm; solution contained 25 mmol l^{-1} glucose, 0.1 mol l^{-1} KCl and 1 mmol l^{-1} phosphate buffer (pH 7.0). Scale bars = 25 μm

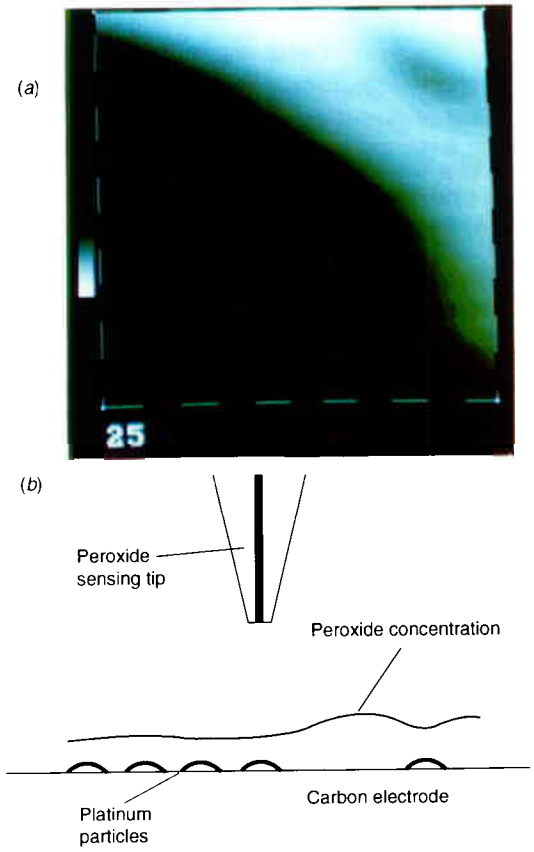

Fig. 14 Image of the concentration profile of hydrogen peroxide near the surface of a glassy carbon–platinum composite electrode.[47] Grey scale indicates the tip current; white corresponds to a high concentration of hydrogen peroxide. Solution contained air-saturated 0.2 mol l^{-1} phosphate buffer (pH 7.0). Potential of the glassy carbon substrate, −1.0 V *versus* silver quasi-reference electrode (AgQRE). Tip-to-surface distance, approximately 20 μm. Scale bars = 25 μm. Image reprinted from ref. 47 with permission. Copyright American Chemical Society

osmium–poly(vinylpyridine) redox polymer to transport electrons from the electrode to the enzyme horseradish peroxidase which is covalently bound to the polymer.[38–40] The current at this microelectrode is proportional to the concentration of hydrogen peroxide for concentrations below approximately 100 μmol l^{-1} and a typical sensitivity is 0.75 A cm^{-2} l mol^{-1}.[47] Again, the tip acts as a passive sensor, monitoring the concentration of hydrogen peroxide near the surface, and the resolution of the images is determined by the diffusion of the analyte from the surface. Fig. 14 shows an example of an image of a C–Pt composite electrode reducing oxygen. The large dark area in the lower left-hand corner shows low hydrogen peroxide concentration over a region of the surface covered with platinum particles which catalyse the decomposition of hydrogen peroxide. The white area corresponds to the bare carbon surface where hydrogen peroxide is a stable intermediate in the reduction of oxygen. The individual platinum particles to the lower left of the image (size of the order of 10 μm) are not resolved because their diffusion layers overlap; however, an isolated particle towards the top right-hand corner is clearly observed. Obviously, the absolute resolution of this technique is much lower than feedback SECM where the resolution is determined by the tip size. However, the selectivity of the biosensor tip is useful in this example, because a platinum tip could not easily distinguish between hydrogen peroxide produced at the bare carbon surface and hydrogen produced by the onset of water reduction at the platinum particles.

Conclusions

The scope and type of applications of SECM continue to grow. The spatial resolution of the technique has attained the tens of nanometres level, and the effective time response for kinetic measurements is now in the microsecond regime. Although wider use has been hindered by the lack of available commercial instrumentation, the unique capabilities of this technique will undoubtedly lead to suitable instruments being produced in the near future.

The support of this research by grants from the Robert A. Welch Foundation and the National Science Foundation is gratefully acknowledged. M. A. acknowledges financial support from the Islamic Development Bank Merit Scholarship Program.

References

1 Bard, A. J., Fan, F.-R. F., and Mirkin, M. V., in *Electroanalytical Chemistry*, ed. Bard, A. J., Marcel Dekker, New York, 1993, vol. 18, p. 243.
2 Bard, A. J., Fan, F.-R. F., and Mirkin, M. V. in *Physical Electrochemistry, Principles, Methods, and Applications*, ed. Rubinstein, I., Marcel Dekker, New York, in the press.
3 Bard, A. J., Fan, F.-R. F., Pierce, D. T., Unwin, P. R., Wipf, D. O., and Zhou, F., *Science*, 1991, **254**, 68.
4 Bard, A. J., Denault, G., Lee, C., Mandler, D., and Wipf, D. O., *Acc. Chem. Res.*, 1990, **23**, 357.
5 Bard, A. J., and Faulkner, L. R., *Electrochemical Methods*, Wiley, New York, 1980, p. 145.
6 Wightman, R. M., and Wipf, D. O., in *Electroanalytical Chemistry*, ed. Bard, A. J., Marcel Dekker, New York, 1989, vol. 15, p. 267.
7 Bard, A. J., Fan, F.-R. F., Kwak, J., and Lev, O., *Anal. Chem.*, 1989, **61**, 132.
8 Mirkin, M. V., Fan, F.-R. F., and Bard, A. J., *J. Electroanal. Chem.*, 1992, **328**, 47.
9 Kwak, J., and Bard, A. J., *Anal. Chem.*, 1989, **61**, 1221.
10 Wipf, D. O., and Bard, A. J., *Anal. Chem.*, 1992, **64**, 1362.
11 Mirkin, M. V., Bulhões, L. O. S., and Bard, A. J., *J. Am. Chem. Soc.*, 1993, **115**, 201.
12 Mirkin, M. V., Richards, T. C., and Bard, A. J., *J. Phys. Chem.*, 1993, **97**, 7672.
13 Wipf, D. O., and Bard, A. J., *J. Electrochem. Soc.*, 1991, **138**, 469.
14 Fleischmann, M., Pons, S., Rolison, D. R., and Schmidt, P. P., *Ultramicroelectrodes*, Datatech Systems, Morgantown, NC, 1987.
15 Hubbard, A. T., and Anson, F. C., in *Electroanalytical Chemistry*, ed. Bard, A. J., Marcel Dekker, New York, 1970, vol. 4, p. 129.
16 Mirkin, M. V., and Bard, A. J., *Anal. Chem.*, 1992, **64**, 2293.
17 Mirkin, M. V., and Bard, A. J., *J. Electrochem. Soc.*, 1992, **139**, 3535.
18 Albery, W. J., and Hitchman, M. L., *Ring-Disk Electrodes*, Clarendon Press, Oxford, 1971.
19 Unwin, P. R., and Bard, A. J., *J. Phys. Chem.*, 1991, **95**, 7814.
20 Zhou, F., Unwin, P. R., and Bard, A. J., *J. Phys. Chem.*, 1992, **96**, 4917.
21 Treichel, D. A., Mirkin, M. V., and Bard, A. J., submitted for publication.
22 Zhou, F., and Bard, A. J., *J. Am. Chem. Soc.*, 1994, **116**, 393.
23 Hapiot, P., Pinson, J., and Yousfi, N., *New J. Chem.*, 1992, **16**, 877.
24 Evans, D. H., Jimenez, P. J., and Kelly, M. J., *J. Electroanal. Chem.*, 1984, **163**, 145.
25 Mirkin, M. V., Arca, M., and Bard, A. J., *J. Phys. Chem.*, 1993, **97**, 10790.
26 Kwak, J., and Anson, F. C., *Anal. Chem.*, 1992, **64**, 250.
27 Lee, C., and Anson, F. C., *Anal. Chem.*, 1992, **64**, 528.
28 Jeon, C., and Anson, F. C., *Anal. Chem.*, 1992, **64**, 2021.
29 Denuault, G., Frank, M. H. T., and Peter, L. M., *Faraday Discuss.*, 1992, **94**, 23.
30 Denuault, G., Frank, M. H. T., and Peter, L. M., *J. Electroanal. Chem.*, 1993, **354**, 331.
31 Arca, M., Mirkin, M. V., and Bard, A. J., unpublished work.
32 Mirkin, M. V., Fan, F.-R. F., and Bard, A. J., *Science*, 1992, **257**, 364.
33 Mirkin, M. V., Fan, F.-R. F., and Bard, A. J., unpublished work.
34 Ammann, D., *Ion Selective Microelectrodes: Principles, Design and Application*, Springer, New York, 1986.
35 Luo, J. L., Lu, Y. C., and Ives, M. B., *J. Electroanal. Chem.*, 1992, **326**, 51.
36 Davis, J. A., in *International Corrosion Conference Series, Localised Corrosion*, eds. Stochle, R. W., Brown, B. F., Kruger, J., and Agrawal, A., National Association of Corrosion Engineers, Houston, 1974, vol. NACE-3, p. 168.
37 Horrocks, B. R., Mirkin, M. V., Pierce, D. T., Bard, A. J., Nagy, G., and Toth, K., *Anal. Chem.*, 1993, **65**, 1213.
38 Pishko, M., Michael, A. C., and Heller, A., *Anal. Chem.*, 1991, **63**, 2268.
39 Heller, A., *Acc. Chem. Res.*, 1990, **23**, 128.
40 Heller, A., *J. Phys. Chem.*, 1992, **96**, 3579.
41 Abe, T., Lau, Y. Y., and Ewing, A. G., *J. Am. Chem.. Soc.*, 1991, **113**, 7421.
42 Ikariyama, Y., Yamauchi, S., Aizawa, M., Yukiashi, T., and Ushioda, H., *Bull. Chem. Soc. Jpn.*, 1988, **61**, 3525.
43 Cronenberg, C. C. H., and van den Heuvel, J. C., *Biosens. Bioelectron.*, 1991, **6**, 255.
44 Kawagoe, J. L., Nichaus, D. E., and Wightman, R. M., *Anal. Chem.*, 1991, **63**, 2961.
45 Pantano, P., Morton, T. H., and Kuhr, W. G., *J. Am. Chem. Soc.*, 1991, **113**, 1832.
46 Pantano, P., and Kuhr, W. G., *Anal. Chem.*, 1993, **65**, 617 and 623.
47 Horrock, B. R., Schmidtke, D., Heller, A., and Bard, A. J., *Anal. Chem.*, 1993, **65**, 3605.

Paper 3/06502B
Received November 1, 1993
Accepted November 30, 1993